Journal of Chromatography, 476 (1989) 3–19
Elsevier Science Publishers B.V., Amsterdam — Printed in The Netherlands

CHROMSYMP. 1626

FAST SEPARATION OF BIOLOGICAL MACROMOLECULES ON NON-POROUS, MICROPARTICULATE COLUMNS

GERARD P. ROZING* and HEINZ GOETZ
Hewlett-Packard GmbH, Waldbronn Analytical Division, P.O. Box 1280, D-7517 Waldbronn 2 (F.R.G.)

SUMMARY

The use of high-performance liquid chromatographic columns for the separation of proteins and nucleic acids is gradually increasing in biochemical laboratories. The efficiency of these columns for such separations has been much lower than that achievable for the separation of smaller molecules. Non-porous microparticulate packings are the logical answer one arrives at after consideration of the chromatographic behaviour of proteins. Non-porous stationary phases are described for the separation of proteins, peptides and nucleic acids. The stationary phases used are TSK-Gel NPR-C_{18}, TSK-Gel NPR-DEAE, TSK-Gel NPR-SP and HYTACH MicroPell C_{18}. A number of fundamental properties of columns based on these sorbents were evaluated, such as permeability, retention behaviour towards small and large molecules, load capacity and stability. Instrumental requirements for these columns are discussed and some applications described.

INTRODUCTION

High-performance liquid chromatographic (HPLC) separations of mixtures of biological macromolecules, such as proteins, on macroporous, microparticulate packings seem to be much poorer than the separation of mixtures of small molecules on the same column material. The lower performance is reflected in the increased zone broadening of the sample components and, therefore, in reduced efficiency and resolution. At the same time, only a much lower speed of separation is possible and longer separation times are necessary than for small-molecule separations.

HPLC separations of biological macromolecules on macroporous, microparticulate supports suffer from a few additional limitations relative to small molecule separations. Recovery of mass and/or biological activity is not quantitative in many instances. The mechanism of separation of macromolecules is not yet understood[1] as well as that of small molecules. Finally, the reproducibility of separations from column to column, even for the same brand of stationary phase, is much poorer in protein separations than for small-molecule separations. Reasons for all these problems can be classified as kinetic factors and thermodynamic factors.

0021-9673/89/$03.50

Kinetic factors

It should be emphasized that for zone broadening to be minimal, the reduced velocity, v ($v = ud_p/D_i$, where u is the velocity of the mobile phase, d_p is the particle size and D_i is the diffusion coefficient of the solute molecule in the mobile phase), must be optimum. Now, if the diffusion coefficient of the solute decreases, because of its higher molecular weight (MW) and/or because diffusion is hindered, the reduced velocity increases. Thus, if the flow-rate through the column, and therefore the mobile phase velocity u, are maintained at typical values for small-molecule separations, the reduced velocity will be too high to achieve optimum values of v for separations of high-molecular-weight substances. Counteracting this by reducing the linear velocity reduces zone broadening, but at the expense of a longer residence time of the solute with adverse consequences for separation time and recovery.

Although it is clear that, for the successful separation of biological macromolecules on HPLC materials, the pores must be enlarged (to >300 Å), it should be pointed out that in many instances this will not be sufficient. The simple concept that biological macromolecules will assume a globular shape and therefore have a minimum surface/volume ratio is not valid in practice. Proteins have particular shapes, which are required for their biological functions, *e.g.*, phosphorylase *b* has a rectangular prism shape of $6.3 \times 6.3 \times 11.6$ nm^2. Therefore, the orientation of the macromolecule relative to the topography of the pore will have a large influence on its diffusion into the pores. Moreover, when the distance between the binding sites on the molecule and the interface decreases, the path of approach may become highly energetic, because the molecule has to be deformed for good binding.

Thermodynamic factors

In addition to kinetic causes, slow binding can be due to chemical reasons. A number of ancillary equilibria will play a role in the overall binding process, and each of these will have its own time requirement. In addition, large molecules will have multiple, similar interactions with the stationary phase and interactions of a different nature due to the heterogeneity of the stationary phase. Further, as it is the aim of a chromatographic separation of, *e.g.*, proteins to separate as much mass as possible, a high load capacity is desirable. This is achieved by improving the phase ratio of the stationary phase by increasing the surface area and ligand density. However, as a consequence, the number of solute–surface interactions increases, with detrimental effects on zone broadening.

Finally, in addition to all the solute–surface interactions, the macromolecules show many conformational and secondary chemical equilibria in the dissolved state. All these conformers and states have their own kinetics and constants of binding, in addition to time requirements for their interconversion. Hence more terms contribute to the overall broadening process than with small molecules.

A chromatographic approach that obviates these disadvantageous processes is the reduction of particle size, which counteracts the increase in reduced velocity. One could imagine pores that have an "infinite diameter" in addition to surfaces that are convex rather than concave, so that the steric hindrance during surface binding is minimized. Reduction of the phase ratio will minimize the number of interactions, while increased temperature will speed up the attainment of equilibria so that the

effects of slow kinetics in the sorption–desorption processes and in the mobile phase equilibria are minimized. Moreover, the favourable geometry of the packing material will also allow a much better coating of the stationary phase to provide a more homogeneous layer with uniform retention.

Non-porous, microparticulate packings have the potential to provide these improvements, especially when they are used at elevated temperature[3–12]. However, a number of questions arise concerning the applicability of these materials to HPLC separations of macromolecules. Reduction of the particle size will have consequences for the permeability of the columns and the column pressure drop. Does this become a practical limitation? Even if the design of the stationary phase is simple, does this help in understanding the separation mechanism better? Is the load capacity of these materials sufficient? What is the lifetime of these columns when they are operated at elevated temperature? What are the instrumental requirements for operating these columns successfully? Finally, for what kind of applications are these columns useful?

The purpose of this work was to investigate the applicability of non-porous, microparticulate columns to the separation of proteins, peptides and nucleic acids, together with the questions formulated above. In addition, a number of practical examples are described.

EXPERIMENTAL

Materials

All experiments were carried out on an HP 1090 Series M LC (Hewlett-Packard, Waldbronn, F.R.G.), equipped with a binary DR5 solvent-delivery system, a variable-volume injector with a 25- or a 250-μl loop installed, and equipped with a cooled sample compartment, a thermostated column compartment with integrated mobile-phase preheater (capillary 100 mm × 0.12 mm I.D., cast in the aluminium heater block). The built-in diode-array detector had a heat exchanger (capillary 550 mm × 0.12 mm I.D., cast in an aluminium block mounted on the detector sheet metal parts and a short 0.12 mm I.D. capillary cast in a small aluminium block mounted on the side of the flow cell) in front of the flow cell. The detection wavelength was set at 214 nm with a band width of 4 nm and the reference wavelength was set at 450 nm with a band width of 100 nm, unless stated otherwise. Control of the chromatographic system and data evaluation were achieved with Series HP 79994A Chemstation computer software.

The columns used were TSK-Gel NPR-C_{18}, -DEAE and -SP (35 mm × 4.6 mm I.D.), packed with 2.5-μm particles (Tosoh, Yamaguchi, Japan) and HYTACH MicroPell C_{18} (30 mm × 4.6 mm I.D. and 75 mm × 4.6 mm I.D.), packed with 1.5-μm particles (Glycotech, New Haven, CT, U.S.A.). For comparison, a 5-μm, 300-Å pore size VYDAC TP C_{18} column (250 mm × 4.6 mm I.D.) (Separations Group, Hesperia, CA, U.S.A.) and a TSK-Gel 5PW-SP column (75 mm × 7.5 mm I.D.), 10 μm, were used. All columns except the MicroPell columns were obtained from Hewlett-Packard.

TSK-gel is a non-porous, polymeric material, based on the well known PW material from Tosoh, which is a hydrophilic polymer. The NPR-PW gels are modified with the same coatings that are available in the porous 4PW and 5PW series, such as octadecyl, diethylaminoethyl and sulphopropyl for reversed-phase, weak anion-

exchange and strong cation-exchange chromatography, respectively[6]. HYTACH MicroPell C_{18} is a non-porous silica-based material which is modified by conventional coating procedures with materials having the octadecyl functionality. This material has been described in detail by Kalgathi and Horváth[12].

Details of experimental conditions are given in the Figure legends.

Ribonuclease A (RNAse), insulin (INS), lysozyme (LYS), bovine serum albumin (BSA) and ovalbumin (OVA) were purchased from Sigma (Deisenhofen, F.R.G.) and used without further purification. DNA restriction fragments were purchased from New England Biolabs (Schwalbach, F.R.G.).

The isocratic column test was carried out with a standard test sample containing dimethyl phthalate (DMP), diethyl phthalate (DEP), biphenyl (BP) and *o*-terphenyl (*o*-TER), 0.1% (w/v) in methanol.

Trifluoroacetic acid (TFA) used in the mobile phase was of Sequanal grade from Pierce (Rockford, IL, U.S.A.). All buffer salts were of analytical-reagent grade and obtained from E. Merck (Darmstadt, F.R.G.). Water used for the mobile phases was purified with an HP 661 water purification system (Hewlett-Packard). All other solvents for mobile phase preparation were of chromatographic grade.

Methods

Phototropically grown cells from the photosynthetic purple bacterium *Rhodopseudomonas viridis* were broken by sonification (buffer: 20 m*M* Tris–HCl–0.1% EDTA–0.02% sodium azide, pH 7.0, 4°C). After centrifugation for 40 min at 16 000 *g*, the samples were adjusted to pH 5 by addition of 2 *M* HCl for cation-exchange chromatography. The samples were centrifuged for 5 min at 1500 *g* prior to injection on to the column.

A 1-mg amount of recombinant human interferon was incubated with L-1-tosylamide-2-phenylethyl chloromethyl ketone (TCPK)-treated trypsin (Sigma) in 0.1 *M* ammonium hydrogencarbonate buffer–0.01 *M* calcium chloride (pH 8) at 37°C for 8 h using an enzyme/protein ratio of 1:30 (w/w). The reaction was stopped by adjusting the pH of the solution to 2 with 1 *M* hydrochloric acid.

RESULTS AND DISCUSSION

Separation performance

Fig. 1a and b illustrate the separation efficiency that can be achieved with non-porous, microparticulate columns. Both chromatograms were obtained with the 35 × 4.6 mm I.D. TSK-Gel NPR-C_{18} column. The resolution in Fig. 1a is very high, so that by increasing the flow-rate and gradient speed, a much faster separation is possible. These conditions were chosen in Fig. 1b. The peak widths at the base are 3–5 s.

The real separation power of this type of column is illustrated in Fig. 2. Here, identical elution conditions were used for the separation of the protein test mixture on a TSK-Gel NPR-C_{18} column and on a macroporous, reversed-phase type of column (VYDAC C_{18}, 5 μm, 250 mm × 4.6 mm I.D.). Although a comparable speed of separation and zone broadening are achieved on the VYDAC column, the resolution is much better on the NPR column. Moreover, in Fig. 2b, BSA starts to show broadening due to some of the factors described in the Introduction. The combined effect of the

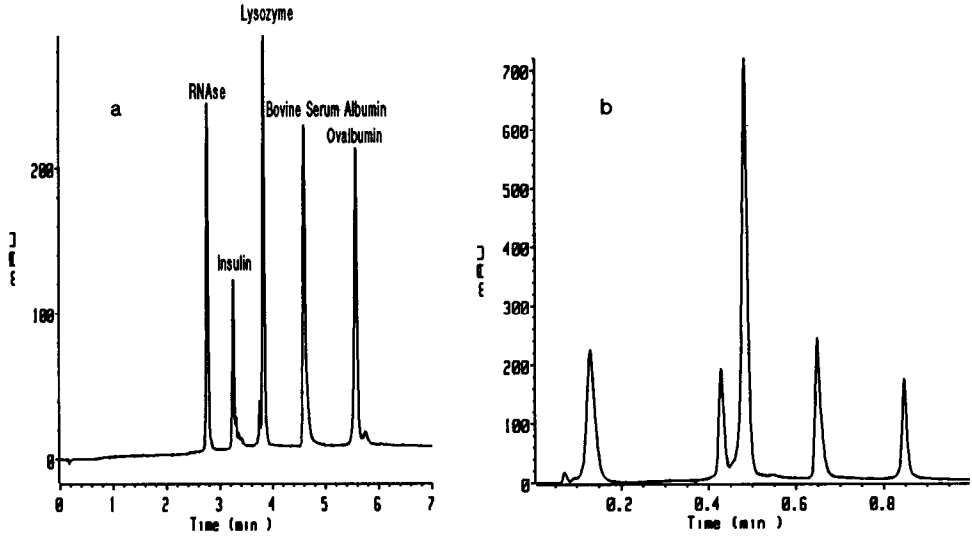

Fig. 1. Fast reversed-phase separation of protein test mixture on TSK-Gel NPR-C_{18} column by gradient elution. Column, 35 × 4.6 mm I.D., 2.5 μm; injection volume, 2 μl (1 mg/ml of each protein); eluent A, 0.1% aqueous TFA; eluent B, 0.1% TFA in acetonitrile. (a) Flow-rate, 1.5 ml/min; gradient from 10 to 60% B in 10 min; column temperature, 40°C. (b) Flow-rate, 3.0 ml/min; gradient from 20 to 60% B in 0.4 min; column temperature, 80°C.

low volume of the NPR column and the intrinsic efficiency of the small particles is responsible for the improved performance. Comparable resolution can be obtained on the VYDAC column, but at a much lower gradient speed.

In Fig. 3, a similar comparison is made between a non-porous and a porous strong cation exchanger (TSK-Gel 5PW-SP, 75 mm × 7.5 mm I.D., 10 μm *vs.*

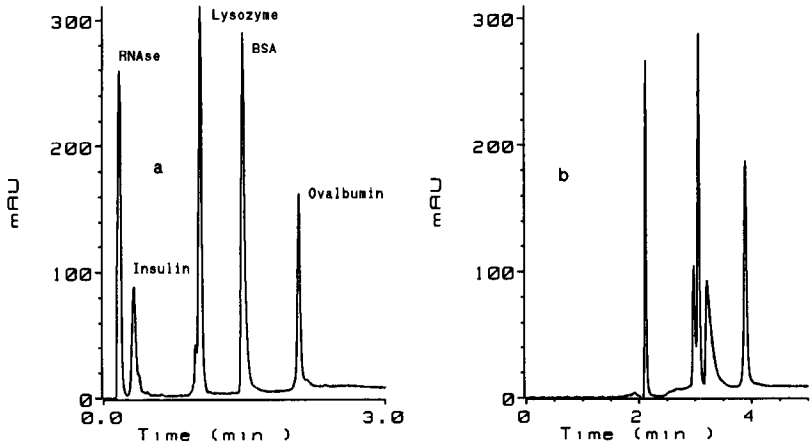

Fig. 2. Comparison of fast reversed-phase gradient elution of protein test mixture on TSK-Gel NPR-C_{18} and VYDAC C_{18} columns. Experimental conditions as in Fig. 1, except flow-rate, 1.5 ml/min; gradient from 27.5 to 57.5% B in 2 min; column temperature, 40°C. (a) Column, TSK-Gel NPR-C_{18}, 35 × 4.6 mm I.D., 2.5 μm; (b) column, VYDAC C_{18}, 250 × 4.6 mm I.D., 5 μm.

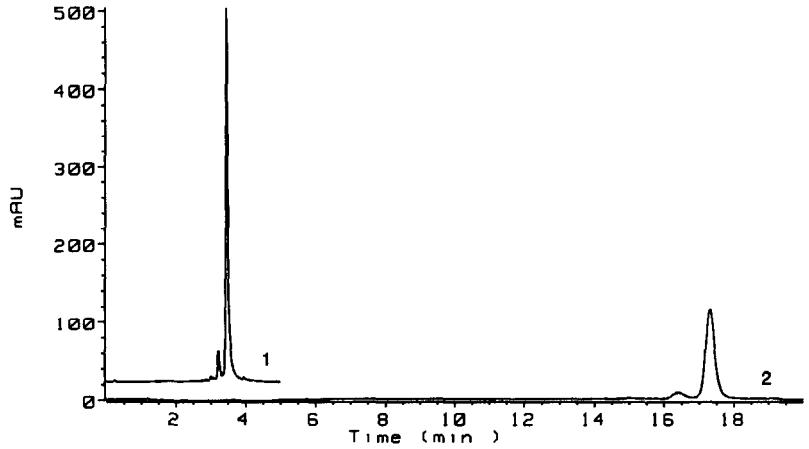

Fig. 3. Purification of a crude lysozyme preparation on porous and non-porous TSK-Gel Sulfopropyl columns. Flow-rate, 1.0 ml/min; eluent A, 0.02 *M* aqueous KH_2PO_4 (pH 6); eluent B, same as A but containing 0.5 *M* NaCl; column temperature, 50°C; sample, 4.5 μg crude lysozyme. (1) Column, TSK-Gel NPR-SP, 35 × 4.6 mm I.D., 2.5 μm; gradient from 0 to 100% B in 5 min; (2) column, TSK-Gel 5PW-SP, 75 × 7.5 mm I.D., 10 μm; gradient from 0 to 100% B in 20 min.

TSK-Gel NPR-SP, 35 mm × 4.6 mm I.D., 2.5 μm). A crude lysozyme preparation was used as a test sample. A five-fold improvement in separation speed and in peak height (solute concentration) is obtained through the combined effect of the low volume of the NPR column, faster gradient and intrinsic efficiency of the packing material. At the same time, it may be observed that the selectivity of the NPR packing is identical with that of the porous support, as illustrated by the elution of the impurities in front of the main peak.

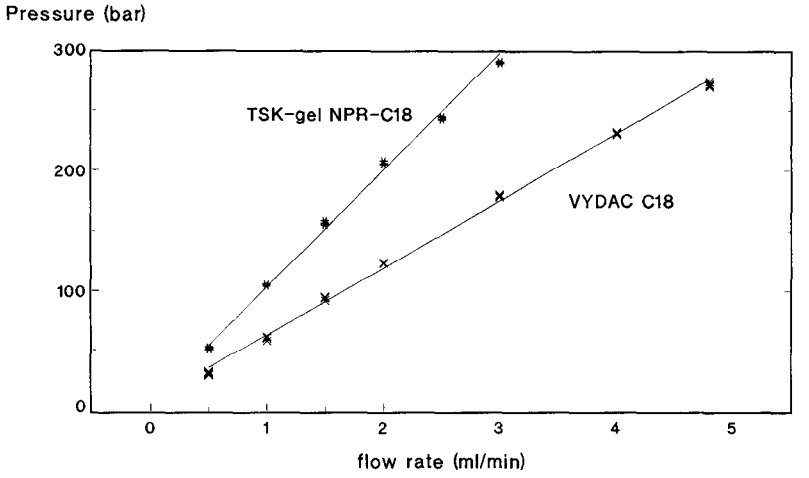

Fig. 4. Column pressure *vs.* flow-rate. Mobile phase, acetonitrile; temperature, ambient. *, TSK-Gel NPR-C_{18} column, 35 × 4.6 mm I.D., 2.5 μm; regression coefficient, 0.9973, permeability, 0.0032 μm^2; column resistance factor, 1950. ×, VYDAC C_{18} column, 250 × 4.6 mm I.D., 5 μm; regression coefficient, 0.9980; permeability, 0.0339 μm^2; column resistance factor, 737.

Column permeability

The permeability of the TSK-Gel NPR-C_{18} column was calculated by the Darcy equation[13] from the slope of the plot of column pressure *vs.* flow-rate (Fig. 4). For reference, the permeability of a VYDAC C_{18} column was obtained in the same way. VYDAC C_{18} is a porous, silica-based reversed-phase material. The column permeability was normalized as the dimensionless column resistance factor. This eliminates the influence of particle size on the permeability and allows the assessment of the influence of packing density and particle shape.

Values of the column resistance factor between 500 and 700 are regarded as optimum for spherical particles[14]. The VYDAC column showed an almost optimum value of 737. The TSK-Gel NPR C_{18} column showed a value three times higher. There may be several reasons for this result, *e.g.*, presence of fines, a smaller nominal particle size or a reduction of the interparticulate space. The last reason proved to be the correct one, as is illustrated in the scanning electron microscope (SEM) picture of particles from an unpacked column in Fig. 5. Some particles have been squeezed together so that only a minimal interparticulate space remained. However, the pressure–flow curve is linear, and no hysteresis was observed. This indicates a very stable column bed, and this was corroborated by the results of the stability tests.

Separation of small molecules

We were interested in verifying whether the high separation efficiency of the TSK-Gel NPR-C_{18} column for proteins could also be useful for small-molecule separations. For this purpose, a simple isocratic column test was carried out, and the result was compared with that for the VYDAC C_{18} and the HYTACH Micro-Pell C_{18} columns (Fig. 6).

The VYDAC column showed excellent efficiency for the four aromatic test solutes (Fig. 6b). Obviously, a lower organic solvent content of the mobile phase is needed in order to achieve a retention on the NPR columns comparable to that on the VYDAC column (8% and 30% acetonitrile *vs.* 70% acetonitrile). However, the peak

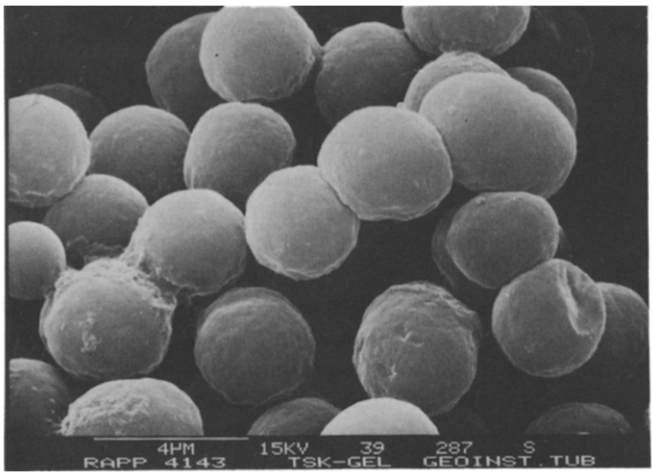

Fig. 5. Scanning electron micrograph of TSK-Gel NPR-C_{18} particles after unpacking a column.

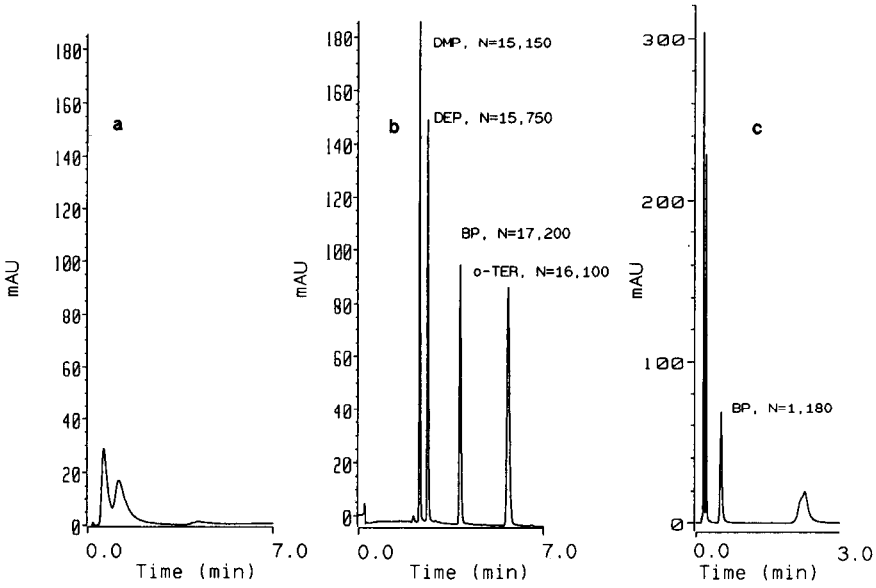

Fig. 6. Comparison of column performance with low-molecular-weight solutes. Flow-rate, 1.5 ml/min; sample, isocratic test sample; injection volume, 1 μl; detection, 254 nm; column temperature, 40°C. (a) Column, TSK-Gel NPR-C_{18}, 35 × 4.6 mm I.D., 2.5 μm; eluent 8% aqueous acetonitrile. (b) Column, VYDAC C_{18}, 250 × 4.6 mm I.D., 5 μm; eluent, 70% aqueous acetonitrile. (c) Column, HYTACH MicroPell C_{18}, 30 × 4.6 mm I.D., 1.5 μm; eluent, 30% aqueous acetonitrile.

shape was very poor and only two peaks were eluted on the TSK-Gel NPR-C_{18} column (Fig. 6a).

Our interpretation is that only DMP and DEP were eluted and that the BP and *o*-TER peaks were broadened so much that they were indistinguishable from the baseline. This is indicative of very poor kinetics of partitioning for the small molecules. The poor kinetics can be caused by the presence of small cracks in the NPR beads or by intercalation of the small-solute molecules in the reticular structure of the polymer. Whatever reason applies, larger molecules will not be subject to these problems and will partition only at the outside of the particle.

In contrast to this observation, the HYTACH MicroPell C18 columns showed good peak shapes for the first three eluting substances (Fig. 6c). The fourth test analyte, *o*-TER, however, is broadened substantially. Moreover, it is striking that on this column, a relatively high concentration of acetonitrile in the mobile phase compared with the TSK-Gel NPR-C_{18} column is necessary to cause elution. Both observations are consistent with the conclusion that the silica-based NPR material is not really "non-porous" for small solutes.

Load capacity

In order to determine whether NPR columns can be used for the separation of larger amounts of proteins, the mass of the solutes injected was varied systematically (Fig. 7). A two-component sample was prepared, and the sample volume was increased. Two observations were made: first, the band width increases with increased

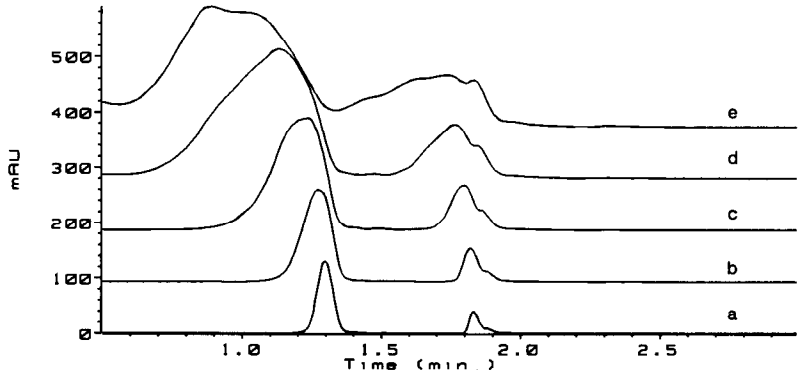

Fig. 7. Load capacity of NPR columns for proteins. Flow-rate, 1.5 ml/min; eluent A, 0.1% aqueous TFA; eluent B, 0.1% TFA in acetonitrile; gradient from 20 to 60% B in 3 min; column, TSK-Gel NPR-C_{18}, 35 × 4.6 mm I.D., 2.5 μm; column temperature, 80°C. (a) Injection volume 5 μl, 13 μg lysozyme, 12 μg BSA; (b) injection volume 10 μl, 26 μg lysozyme, 24 μg BSA; (c) injection volume 20 μl, 52 μg lysozyme, 48 μg BSA; (d) injection volume 40 μl, 104 μg lysozyme, 96 μg BSA; (e) injection volume 75 μl, 195 μg lysozyme, 180 μg BSA.

load, but in a way very similar to the empirical and theoretical models developed by Snyder *et al.*[15] and Ghodbane and Guiochon[16] for small molecules; and second, the small shoulder on the BSA peak stays partly resolved when the load is increased, demonstrating the high efficiency of the column.

The available surface area on the NPR material amounts to 1750 cm^2 per unit column volume (assuming an interparticulate porosity of 0.25). This means that at the lowest load (trace a in Fig. 7) the overall BSA concentration at the surface of the bead is approximately 0.1 pmol/cm^2. Monolayer coverage of BSA on a surface amounts to a surface concentration of 1 pmol/cm^2 (ref. 17). The available stationary phase surface is thus used very efficiently in these columns, providing still reasonable resolution at high load conditions. In fact, the question of load capacity as a stationary phase property becomes relatively unimportant. The proper question to ask for preparative work on these columns is, "how much resolution can be sacrificed in order to improve the throughput?"

Recovery studies

It was expected from the considerations described in the Introduction that NPR columns would show improved recovery. This was verified quantitatively (Fig. 8). The benchmark protein separation was repeated three times, and a blank run was performed immediately afterwards (Fig. 8a and b). As can be seen, a trace of BSA and a relatively large ovalbumin peak were produced. The recovery, based on peak-area measurement, was 64% for ovalbumin. This is corroborated by data published by Kato *et al.*[6]. Ovalbumin is a relatively hydrophobic protein, known to give poor recovery from reversed-phase columns.

The column could be easily cleaned up by injection of glacial acetic acid (Fig. 8c). The low column volume, combined with the low surface area per column, allows for efficient cleaning of the column merely by injection of small volumes of cleaning liquids rather than pumping these, in most instances, very aggressive solvents with the expensive HPLC pump.

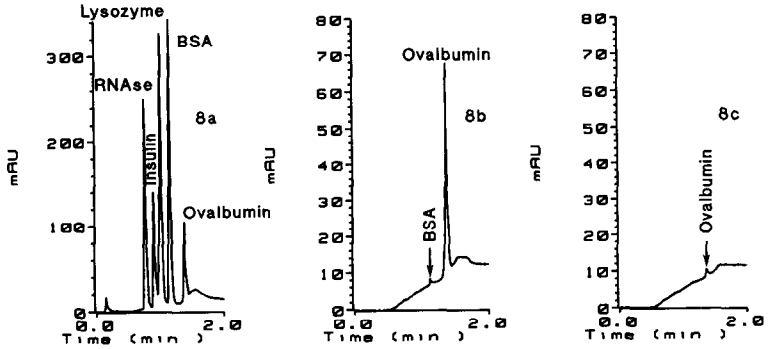

Fig. 8. Protein recovery on NPR columns. Conditions as in Fig. 7, except gradient from 20 to 60% B in 1 min; column temperature, 40°C; sample, protein test mixture; injection volume, 2 μl.

In a separate series of experiments with increased column temperature and increased mobile phase flow-rate, the recovery of ovalbumin was quantitative. These conditions were applied in the precision studies detailed in Table I. Because excellent repeatability of peak heights and peak areas was obtained, it can be asserted that the recovery was quantitative in this test.

Column stability

The elevated temperatures used to operate these columns render the mobile phase highly aggressive, generating concern about the stability of the column bed and also potential bleeding of the C_{18} coating from the bead surface. This would have consequences for the separation efficiency and retention behaviour of the solutes, and bleeding of the coating would contaminate the collected fractions. Therefore, the stability of the columns was investigated. Two procedures were used for the test. In the first, a slow gradient from 10:90 to 90:10 eluent A (0.1% aqueous TFA)–eluent B (0.1% TFA in acetonitrile) at a low flow-rate of 1.0 ml/min was applied at 75°C for 36 h. The efficiency of the column was checked before and after the test (Fig. 9a and b).

TABLE I

QUANTITATIVE PRECISION ON TSK-Gel NPR-C_{18} COLUMN

Experimental conditions: column, 35 mm × 4.6 mm I.D.; flow-rate, 3.0 ml/min; eluent A, 0.1% aqueous TFA; eluent B, 0.1% TFA in acetonitrile; gradient from 20 to 60% B in 2 min; column temperature, 80°C; injection volume, 2 μl; No. of replicates, 9.

Solute	*Relative standard deviation (%)*		
	Retention time	*Peak height*	*Peak area*
RNAse	1.1	2.0	0.5
Insulin	0.1	1.7	7.0
Lysozyme	0.2	1.1	0.4
BSA	0.1	1.3	1.8
Ovalbumin	0.1	1.1	1.3

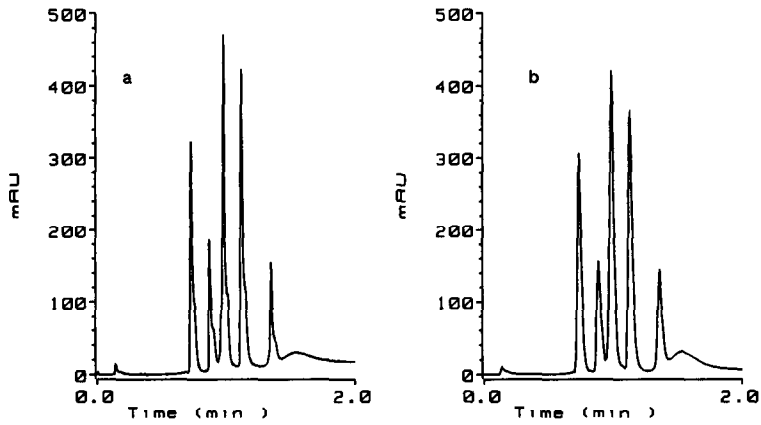

Fig. 9. Stability test of TSK-Gel NPR-C_{18}. Comparison of performance before and after stress test. Stress test conditions: eluent A, 0.1% aqueous TFA; eluent B, 0.1% TFA in acetonitrile; gradient from 10 to 90% B in 90 min; flow-rate, 1.0 ml/min; column temperature, 75°C. Performance test conditions: identical with those in Fig. 8. (a) Starting chromatogram; (b) after 36 h of stress test.

After this test, the same column was operated under faster conditions, with a flow-rate of 1.5 ml/min and a gradient from 80:20 to 40:60 A–B in 3 min, at a column temperature of 80°C, and the protein test mixture was injected continuously (Fig. 10a–c). The overall duration of the test was 7 days, during which time 40 000 column volumes of mobile phase were flushed through the column. As a separation takes 10–20 column volumes to be complete, this is equivalent to 2000–4000 injections. The experiments were carried out with the TSK-Gel NPR-C_{18} column. No sign of column deterioration was observed. The peak shape even improved slightly during the test (compare Fig. 10b and c), whereas none of the peak retention times changed significantly.

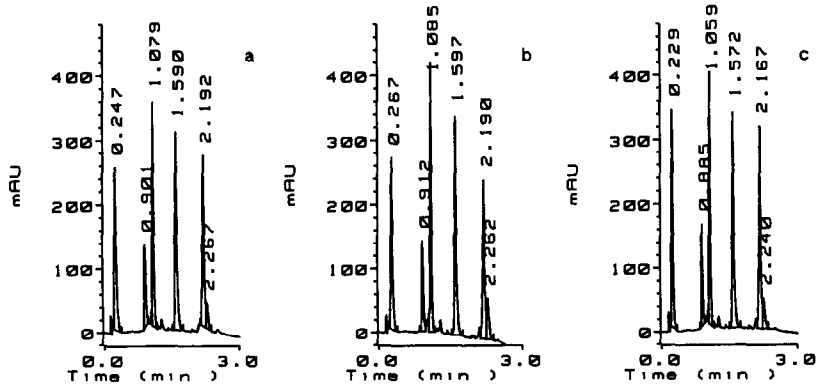

Fig. 10. Stability test of TSK-Gel NPR-C_{18} by repetitive injection of the protein test mixture. Conditions as in Fig. 7, except test sample, protein test mixture; injection volume, 2 μl. (a) First injection; (b) after 186 injections; (c) after 311 injections.

Instrumental requirements

The low column volume and high intrinsic efficiency of the NPR columns place strict demands on the instrumentation used to operate these columns successfully. A number of these requirements were investigated here.

It has been reported[18] that mere thermostating of HPLC columns at high temperature is inadequate. The large temperature difference between the incoming mobile phase and the column itself readily destroys the separation efficiency because of the temperature gradients that are generated. This can be overcome by heating the mobile phase to the column temperature prior to entering the column. Most modern HPLC instruments provide this facility. The effect of omitting mobile phase preheating is demonstrated in Fig. 11. The expanded part of the trace shows the ovalbumin peak, which is doubled in Fig. 11b (as are all the other peaks).

After leaving the column, the temperature of the mobile phase will be substantially different from the temperature of the detector flow cell. As a consequence, temperature-mediated refractive index effects will be transmitted to the detector, leading to apparent light absorption and noise. This is illustrated in Fig. 12b. Efficient mobile phase thermostating to the temperature in the detector is required. This is achieved by an efficient, dual-stage, passive heat exchanger, which consists of a large stage with a high capacity and a small, fast heat exchanger, mounted directly on the flow cell to eliminate fast, low-amplitude temperature fluctuations. The beneficial effect of this adjustment is seen in Fig. 12a. The noise in this instance is down to 0.1 mAU, whereas without thermostating a 20–50-fold higher noise level is observed. The overall volume of this heat exchanger is approximately 6 μl, and no performance loss due to band spreading is observed.

The fast gradients used have consequences for the ability of the pumping system to generate these mobile phase compositions in a reproducible, linear and rapid manner. A low dead volume between the mixing point and the head of the column is required to allow rapid transfer of the gradient profile and to avoid excessive spreading and rounding of the gradient profile. The actual profile was checked by normal HPLC

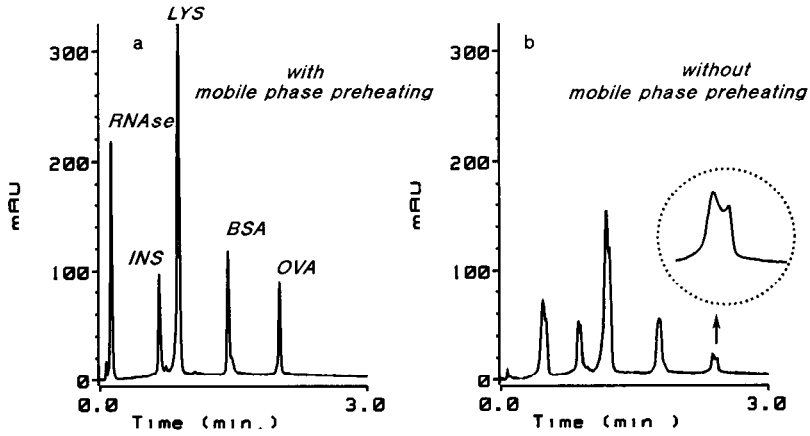

Fig. 11. Influence of mobile phase preheating on column performance. Conditions as in Fig. 7, except test sample is protein test mixture; injection volume, 2 l. (a) With mobile phase preheating; (b) without mobile phase preheating.

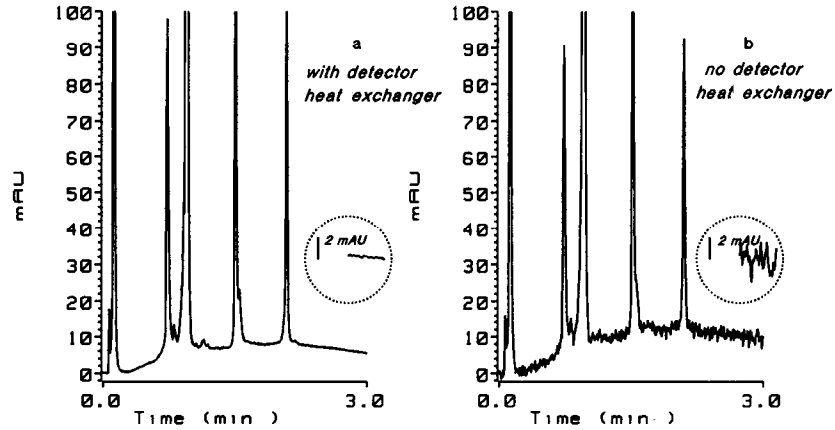

Fig. 12. Influence of mobile phase thermostating on detector performance. Conditions as in Fig. 7, except test sample is protein test mixture. (a) With detector heat exchanger; (b) without detector heat exchanger.

pump performance verification tests in which the TFA was eliminated from eluents A and B, and 0.5% (v/v) acetone was used as a tracer in eluent B. In the pump test no column was used. The profile that is generated now is easily monitored (Fig. 13). A small delay volume, 510 μl, of which *ca.* 300 μl originates from the sample loop, was found. Low rounding at the points where the gradient starts and ends indicates a slight spreading in the delay volume. Even at the highest speed (100% change per minute) the major part of the trace was linear.

Applications

Soluble cytochrome *c*2 is present in the supernatant of the purple bacterium *Rhodopseudomonas viridis*, described under Experimental. Direct injection of 50 μl of the supernatant into a TSK-Gel NPR-SP column allows the isolation of 0.5 μg of the pure cytochrome *c*2 directly (Fig. 14). Previously, chromatographic isolation of this

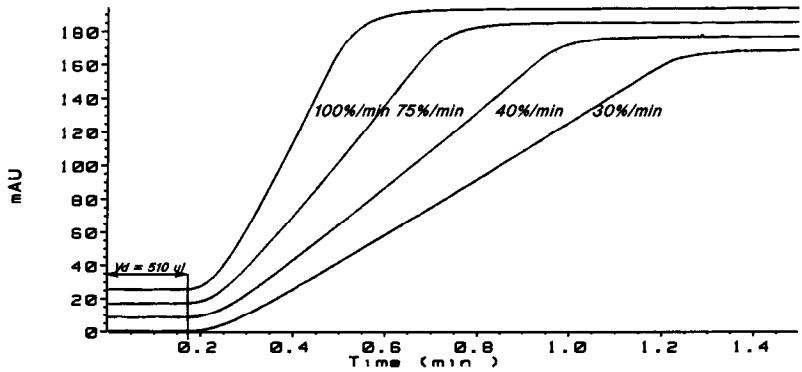

Fig. 13. Demonstration of pump performance for fast gradient elution. Conditions: flow-rate, 3.0 ml/min; eluent A, water; eluent B, 0.5% acetone in acetonitrile; gradient from 27.5 to 57.5% B, without column, detection at 275 nm.

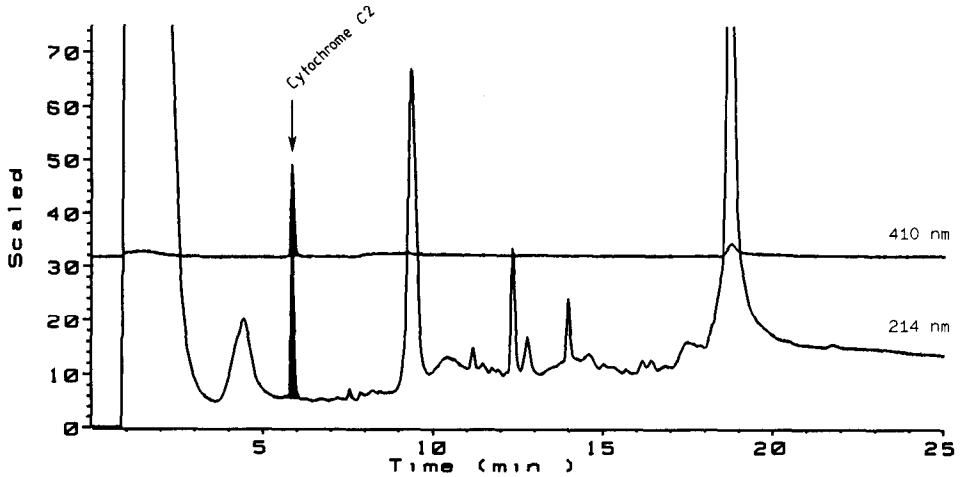

Fig. 14. Isolation of cytochrome *c*2 from the supernatant of a *Rhodopseudomonas viridis* cell culture. Conditions: flow-rate, 1.5 ml/min; eluent A, 0.01 *M* NaH_2PO_4 (pH 5); eluent B, same as A but with 0.5 *M* NaCl; gradient from 0 to 100% A in 20 min; column, TSK-Gel NPR-SP, 35 × 4.6 mm I.D., 2.5 μm; injection volume, 50 μl of supernatant; total protein concentration, 1.5 mg/ml; amount isolated, 0.5 μg cytochrome *c*2.

protein was carried out by low-pressure chromatography on a weak anion-exchange column (Whatman DE-52, diethylaminoethylcellulose), followed by chromatofocusing on a PBE 94 gel with Polybuffer (Pharmacia), and took over 1 day. With the NPR-SP column, the protein was available for further work within a few minutes after centrifugation and injection on to the column.

The structure of small DNA molecules, such as plasmids and viral and bacteriophage DNA, is well known nowadays. Restriction enzymes clip these molecules and provide fragments that are known exactly. These fragments serve as

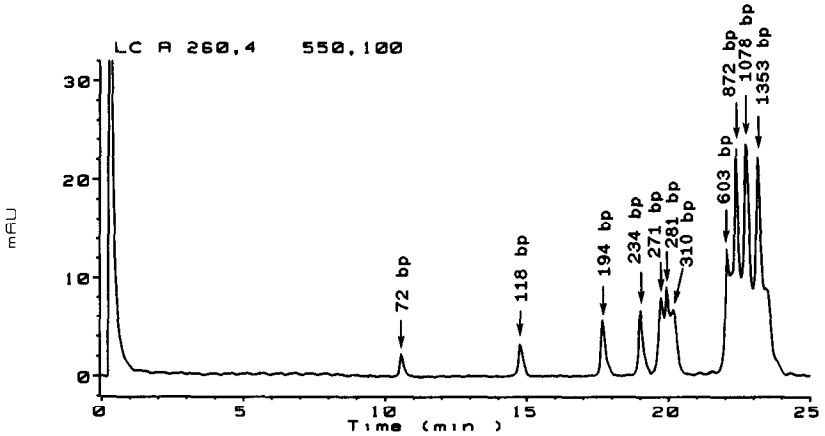

Fig. 15. Separation of restriction fragments of φX174 RF Phage DNA digested with HaeIII. Conditions: flow-rate, 0.9 ml/min; eluent A, 6 *M* urea in 0.03 *M* NaH_2PO_4 (pH 6); eluent B, same as A but with 1 *M* NaCl; gradient from 30 to 50% B in 25 min; column, TSK-Gel NPR-DEAE, 2.5 μm, 35 × 4.6 mm I.D.; injection volume, 10 μl (1 mg/ml). bp = base pairs.

molecular-weight markers in the electrophoresis of unknown DNA restriction fragments. The potential of NPR-DEAE columns for separating high-molecular-weight nucleotides was illustrated with these fragments (Fig. 15). A salt gradient with a high concentration of urea in the mobile phase suffices to obtain an excellent separation of all the fragments present in the sample. In fact, electrophoresis showed the separation of only eight fragments whereas the HPLC analysis showed all eleven fragments.

The favourable separation efficiency of these columns can also be used for the rapid separation of peptides[4], as illustrated by Fig. 16. For this work, a longer column having a higher peak capacity, or more chromatographic space for positioning peaks, is required. Therefore, the HYTACH MicroPell C_{18} column (75 × 4.6 mm I.D.) was used for this work and compared with the VYDAC C_{18} column (250 × 4.6 mm I.D.). The top chromatogram (Fig. 16) shows the VYDAC C_{18} column and the analysis of the trypsin digest of genetically engineered human interferon. A gradient of from 0 to 55% in 2 h was applied in order to achieve almost baseline separation of most peptides. The middle trace in Fig. 16 shows the chromatogram of the same sample on the TSK-Gel NPR-C_{18} column. In order to keep the conditions on both columns the same, the gradient time was reduced by the same factor as the ratio of the lengths of the two columns. It can be seen that the number of peaks separated on the NPR-C_{18} column is much smaller than that on the VYDAC column.

A separation that is comparable to that on the VYDAC column was obtained when the tryptic peptide sample was injected into the HYTACH MicroPell C_{18} column and the same gradient range but with a gradient time of 36 min was used. The overall analysis time on this column was 34 min, compared with 100 min on the VYDAC column. In order to obtain a better visual comparison of the separation efficiency and selectivity of the HYTACH column relative to the VYDAC column, the time axis of the lower trace in Fig. 16 was stretched so that the interferon peaks

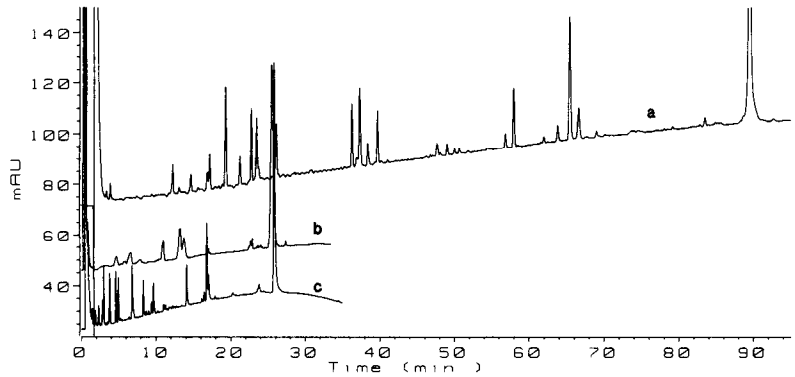

Fig. 16. Comparison of separation performance of non-porous reversed-phase columns with porous reversed-phase columns. Conditions: flow-rate, 1.0 ml/min; eluent A, 0.1% aqueous TFA; eluent B, 0.1% TFA in acetonitrile, gradient from 0 to 55% in 120, 16.8 and 36 min in chromatograms a, b and c, respectively. Sample, recombinant human interferon digested with trypsin as described under Experimental. (a) Column, VYDAC C_{18}, 250 × 4.6 mm I.D., 5 μm; column temperature, 40°C. (b) Column, TSK-Gel NPR-C_{18}, 35 × 4.6 mm I.D., 2.5 μm; column temperature, 40°C. (c) Column, HYTACH MicroPell C_{18}, 75 × 4.6 mm I.D., 1.5 μm; column temperature, 55°C.

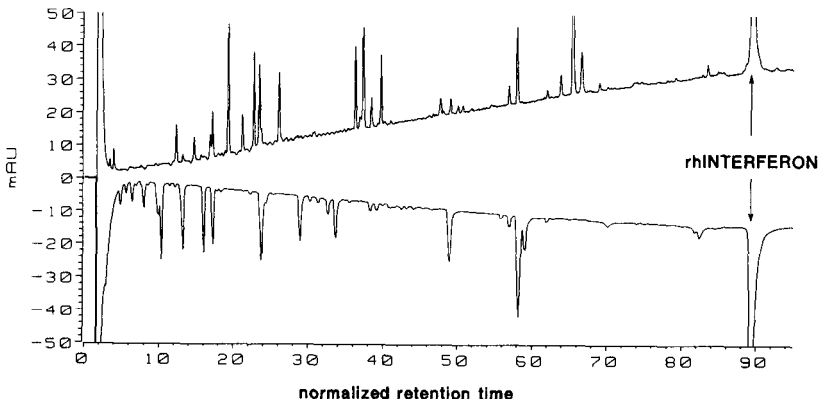

Fig. 17. Comparison of VYDAC and HYTACH MicroPell columns for tryptic map analysis. Conditions as in Fig. 16. Upper trace, VYDAC column; inverse trace, HYTACH MicroPell C_{18} column.

matched in both chromatograms (Fig. 17). As can easily be seen, the same peak clusters can be identified in both traces. However, the relative peak-height ratios within each peak trace are different. This indicates differences in the recoveries from the two columns.

Although the number of major peaks separated was 20 on the MicroPell column and 23 on the VYDAC column, it must be taken into account that the gradient conditions were not fully optimized for the HYTACH column. The excellent reproducibility of this system is illustrated in Fig. 18, which is an overlap of five consecutive runs of the trypsin digest of the interferon sample.

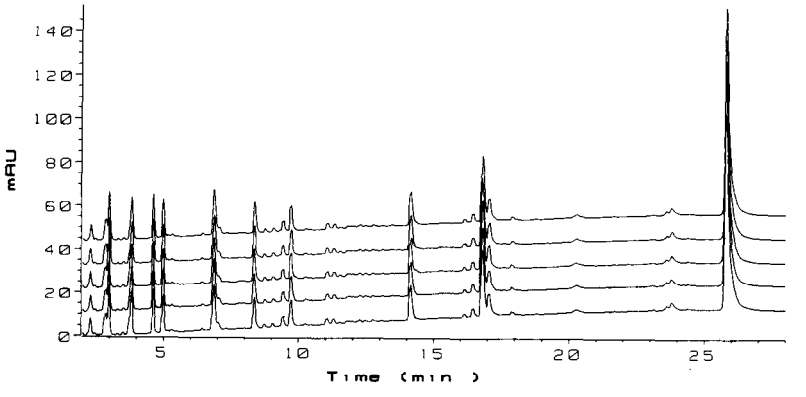

Fig. 18. Five consecutive injections of tryptic digest of rh-interferon onto a HYTACH MicroPell C_{18} column, 75 × 4.6 mm I.D., 1.5 μm. Conditions as in Fig. 16.

CONCLUSIONS

Non-porous, microparticulate columns have considerable potential for rapid, high-resolution separations of proteins. This is effected in short, low-volume, columns operated at elevated temperature. At the same time, the TSK-Gel NPR-C_{18} columns showed excellent bed stability, demonstrated by the linearity of the pressure *vs.* flow-rate curve and by the results of the stability stress test. However, the permeability of these columns needs to be improved. Small molecules permeate the "non-porous" beads, giving rise to poor separations. The applicability of these columns is limited by molecular weight and by molecular structure. High protein loads are feasible while maintaining chromatographic resolution and recovery on the NPR-C_{18} column. If the columns become fouled, they can be easily cleaned by injection of small volumes of a cleaning agent such as acetic acid. Instrumental requirements for operating these columns, although demanding, can be met by modern HPLC equipment.

The main applicability of these columns will be for rapid micropreparative-scale separations (<200 μg), for verification of the homogeneity of recombinant proteins (deamidated forms, mutants and degraded forms) and for fast tryptic mapping. In the last application, on the MicroPell column, the number of resolvable peptides will be limited by the peak capacity of the relatively short column (75 mm).

ACKNOWLEDGEMENTS

The authors acknowledge the help of Dr. Friedrich Lottspeich of the Max Planck Institute for Biochemistry, Munich, F.R.G., in generating some of the chromatograms, Dr. Wolfgang Rapp, Laboratory for Organic Chemistry, University of Tübingen, Tübingen, F.R.G., for generating the SEM picture and Dr. Virginia Curtis, Hewlett-Pachard, Waldbronn, F.R.G., for critically reading the manuscript.

REFERENCES

1 L. R. Snyder and M. A. Stadelius, in Cs. Horváth (Editor), *HPLC — Advances and Perspectives*, Vol. 4, Academic Press, London, 1986, pp. 195–312.
2 N. L. Johnson, N. B. Madsen, J. Mosely and K. S. Wilson, *J. Biol. Chem.*, 90 (1974) 703.
3 J. K. Duncan, A. J. C. Chen and C. J. Siebert, *J. Chromatogr.*, 397 (1987) 1.
4 D. J. Burke, J. K. Duncan, L. C. Dunn, L. Cummings, C. Siebert and G. S. Ott, *J. Chromatogr.*, 353 (1986) 425.
5 D. J. Burke, J. K. Duncan, C. Siebert and G. S. Ott, *J. Chromatogr.*, 359 (1986) 533.
6 Y. Kato, T. Kitamura, A. Mitsui and T. Hashimoto, *J. Chromatogr.*, 398 (1987) 327.
7 Y. Kato, T. Kitamura, A. Mitsui, Y. Yamasaki, T. Hashimoto, T. Murotsu, S. Fukushige and K. Matsubara, *J. Chromatogr.*, 447 (1988) 212.
8 K. K. Unger, G. Jilge, J. N. Kinkel and M. T. W. Hearn, *J. Chromatogr.*, 359 (1986) 61.
9 R. Janzen, K. K. Unger, H. Giesche, J. N. Kinkel and M. T. W. Hearn, *J. Chromatogr.*, 397 (1987) 91.
10 Y. F. Maa and Cs. Horváth, *J. Chromatogr.*, 445 (1988) 71.
11 M. A. Rounds and F. E. Regnier, *J. Chromatogr.*, 447 (1988) 73.
12 K. Kalgathi and Cs. Horváth, *J. Chromatogr.*, 398 (1987) 335.
13 H. Darcy, *Les Fontaines Publiques de la Ville de Dijon*, Dalmont, Paris, 1856.
14 K. K. Unger, *Porous Silica (Journal of Chromatography Library*, Vol. 16), Elsevier, Amsterdam, 1979.
15 L. R. Snyder, G. B. Cox and P. E. Antle, *J. Chromatogr.*, 444 (1988) 303.
16 S. Ghodbane and G. Guiochon, *J. Chromatogr.*, 444 (1988) 275.
17 F. E. Regnier, personal communication.
18 H. Schrenker, *J. Chromatogr.*, 213 (1981) 243.